Differences in ionospheric O$^+$ and H$^+$ outflow during storms with and without sawtooth oscillations

N. Nowrouzi[1,2,3], L. M. Kistler[1,2], K Zhao[4], E. J. Lund[1], C. Mouikis[1], G. Payne[5], B. Klecker[6]

[1]Space Science Center, University of New Hampshire, Durham, NH, USA.
[2]Physics Department, University of New Hampshire, Durham, NH, USA
[3]Center for Space Physics, Boston University
[4]School of Mathematics and Statistics, Nanjing University of Information Science and Technology, Nanjing, China.
[5]University of Colorado Boulder.
[6]Max-Planck-Institut für extraterrestrische Physik, Garching, Germany.

Key Points:

- The intensity and location of O$^+$ outflow during storms are different in storms with and without sawtooth oscillations.
- The peak dayside outflow is significantly shifted towards dawn during storms with sawtooth observations.
- The nightside picture is mixed; the pre-midnight O$^+$ outflow is higher in the main phase but lower in the recovery phase of sawtooth storms.

Corresponding author: Niloufar Nowrouzi, `nowrouzi@bu.edu`

Abstract

Previous simulations have suggested that O^+ outflow plays a role in driving the sawtooth oscillations. This study investigates the role of O^+ by identifying the differences in ionospheric outflow between sawtooth and non-sawtooth storms using 11 years of FAST/Time of flight Energy Angle Mass Spectrograph (TEAMS) ion composition data from 1996 through 2007 during storms driven by coronal mass ejections (CMEs). We find that the storm's initial phase shows larger O^+ outflow during non-sawtooth storms, and the main and recovery phases revealed differences in the location of ionospheric outflow. On the pre-midnight sector, a larger O^+ outflow was observed during the main phase of sawtooth storms, while non-sawtooth storms exhibited stronger O^+ outflow during the recovery phase. On the dayside, the peak outflow shifts significantly towards dawn during sawtooth storms. This strong dawnside sector outflow during sawtooth storms warrants consideration.

Plain Language Summary

A sawtooth event is a convection mode in Earth's magnetosphere, which transports solar wind plasma and energy into the inner magnetosphere and ionosphere. Despite three decades since their discovery, the mechanism behind sawtooth oscillations remains uncertain. One theory suggests that O^+ outflow induces sawtooth oscillations through an internal feedback mechanism. In line with this theory, some simulations have generated sawtooth oscillations under steady geomagnetic conditions. Furthermore, previous observations indicate that some, but not all, geomagnetic storms exhibit sawtooth oscillations. This study utilizes data from the FAST/TEAMS instrument (1996-2007) and compares O^+ outflow variations during geomagnetic storms with and without sawtooth oscillations. Findings indicate that during the storms' initial phase, sawtooth storms produce less O^+ outflow than non-sawtooth storms. Additionally, non-sawtooth storms exhibit higher O^+ outflow in the dayside during the main phase and in the pre-midnight sector during the recovery phase, challenging the key role of O^+ outflow in driving the feedback mechanism. However, observing large O^+ outflow in the dawnside sector of sawtooth events suggests more investigation is needed.

1 Introduction

When the interplanetary magnetic field (IMF) is southward, magnetotail reconnection brings solar wind plasma and energy into the inner magnetosphere and ionosphere via three different modes: Steady Magnetospheric Convection mode(SMC), magnetic substorms, and the comparatively less-explored phenomenon of sawtooth events. In SMC, the magnetosphere does not accumulate solar wind energy but redirects it from the dayside to the nightside by a nearly balanced reconnection rate on both sides (Sergeev et al., 1996; DeJong et al., 2008). Conversely, during the magnetospheric substorm, the magnetosphere acts as an energy reservoir, storing solar wind energy in the tail lobes and then releasing it into the inner magnetosphere and ionosphere. For an isolated substorm, the process of loading/unloading energy is localized near midnight in magnetic local time (MLT) (Russell & McPherron, 1973; Hones Jr. et al., 1984). In some cases, this loading/unloading energy occurs over a wider MLT region, during a longer time period, and quasi periodically with more than two oscillations. This mode is termed a global sawtooth event (Reeves et al., 2002; Henderson, 2004). The reason for the magnetosphere's preference for one mode over the other in response to the solar wind energy input is still unknown.

Global sawtooth events, identified as quasi-periodic, large-amplitude oscillations in energetic particles at geosynchronous orbit (Belian & Cayton, 1989; Borovsky et al., 1993) with a periodicity of 2–4 hours (Cai & Clauer, 2009), derive their name from the saw blade-like characteristics of particle injections marked by a gradual decrease (growth

phase) followed by a sharp increase (onset) (Belian et al., 1995). These energetic particle flux oscillations are correlated with magnetic field changes in the tail, at geostationary orbit, and ground stations, as well as changes in the auroral electrojet index, auroral precipitation, and polar cap indices (Huang et al., 2003; Kitamura et al., 2005; Cai et al., 2006; Henderson et al., 2006; Huang & Cai, 2009; Troshichev & Janzhura, 2009). These observations suggested that the sawtooth mode is generated by an internal magnetospheric instability (Huang, 2011); however, there are studies that claim sawtooth events are generated by external parameters in solar wind drivers (Lee et al., 2004, 2006; Cai & Clauer, 2013). Cai and Clauer (2009, 2013) compiled a comprehensive list of sawtooth events spanning from 1996 to 2007, encompassing a total of 126 events. Cai et al. (2011), through extensive statistical analysis, examined the relationship between sawtooth events and geomagnetic storms and found that a substantial majority, 94.6%, of sawtooth events occurred during geomagnetic storms.

During geomagnetic storms, the O^+ density and pressure and its occurrence frequency in the plasma sheet and lobe are enhanced (Kistler et al., 2006, 2010; Liao et al., 2010). The ionosphere is the main source of O^+ ions in the magnetosphere (Shelley et al., 1972; Sharp et al., 1974), predominantly from two regions: the dayside cusp and the nightside auroral region (Yau & André, 1997) and the increase of O^+ outflow during storms has been reported from both sources e.g. (Yau et al., 1988; Cully et al., 2003; Nowrouzi et al., 2023). Cusp-origin O^+ flows along the open field lines to the lobe and enters the plasma sheet during reconnection in the tail. The field lines in the nightside auroral regions are directly connected to the plasma sheet. The occurrence of sawtooth events during storms, when O^+ is enhanced, suggests that the cause of substorms may be related to the O^+.

Brambles et al. (2011) incorporated ionospheric O^+ fluence into the multifluid Lyon-Fedder-Mobarry (LFM) model (Lyon et al., 2004) and demonstrated that strong O^+ fluence can generate sawtooth events in simulations. Ouellette et al. (2013) investigated the mechanism for driving the events and introduced a hypothesis for the periodicity of sawtooth events: the periodic loading and unloading of O^+ ions through ionospheric outflow into the plasma sheet changes the reconnection rate within the magnetotail current sheet. These variations in reconnection rate lead to distinct magnetic field configuration changes in the tail, releasing an O^+-rich plasmoid and sending particle precipitation and Alfvénic waves towards the ionosphere, which drives more outflow for the subsequent sawtooth in the cycle. This mechanism suggests that it is nightside O^+ outflow that is responsible. Using simulation Brambles et al. (2013) found that for an event driven by coronal mass ejections (CME) with steady solar wind conditions, nightside O^+ fluence was required to generate the sawtooth oscillations. In contrast, sawtooth events driven by streaming interaction regions (SIR) could be driven without O^+ fluence. Using a physics-based model, Varney et al. (2016) simulated a sawtooth event under steady solar wind conditions and found that the cases that developed sawtooth oscillations had strong outflow in the midnight auroral region. Zhang et al. (2020) investigated whether cusp outflow could also drive sawtooth oscillations. They found that while only 10% of dayside cusp O^+ outflow reached the plasma sheet, it was sufficient to induce sawtooth oscillations. Finally, Wang et al. (2022) showed that kinetic reconnection in the magnetotail can reproduce the periodic loading and unloading of the magnetic flux in the magnetosphere even without ionospheric outflow. Thus, from the simulation results, sawtooth oscillations can be driven by either nightside or dayside outflow or from strong driving, independent of outflow.

The magnetotail observations also do not give a clear picture. Liao et al. (2014) investigated and compared the composition of the plasma sheet during sawtooth events and isolated storm-time substorms. While the O^+/H^+ ratio was higher on average during the sawtooth substorms, there were substorms with a high O^+/H^+ ratio for no sawtooth events, as well as sawtooth substorms with a low O^+/H^+ ratio.

Regarding the source of the O^+ nightside aurora outflow vs. dayside cusp outflow during the sawtooth substorms, an observational study showed that the cusp is the predominant source of O^+ ions in the 15-20 Re plasma sheet where sawtooth events driven by SIRs and CMEs (Lund et al., 2018). This is where the near-Earth neutral line is typically located, therefore, where the plasma sheet composition would potentially affect reconnection.

Therefore, neither the simulations nor the observations have been conclusive on the role of O^+ in driving sawtooth oscillations. However, another aspect that might help to clarify the role of O^+ is to determine how the ion outflow varies in intensity and location between storms with sawtooth oscillations and storms without. Since global sawtooth oscillations occur during some, but not all geomagnetic storms (Borovsky, 2004), it is worthwhile to investigate the variation of ionospheric O^+ outflow during CME storms, comparing those with sawtooth events to those without sawtooth events. If either dayside or nightside O^+ outflow is involved in triggering sawtooth events, we would expect significant differences in the outflow characteristics for these two types of events. Since most of the sawtooth teeth occur in the main and recovery phases (Cai et al., 2011), the outflow characteristics are investigated during different storm phases.

2 Data and Methodology

To examine the role of ionospheric O^+ outflow in driving sawtooth events, this study measures the averaged ionospheric O^+ and H^+ outflow during geomagnetic storms and compares the outflow during sawtooth storms (i.e., storms with sawtooth oscillations) with the outflow during non-sawtooth storms. For this purpose, we will use the list of all CME storms with clear main and recovery phases and with a minimum value of Disturbance storm time index (Dst) less than $-50nT$, from 1996 to 2007, published in Nowrouzi et al. (2023). This list contains information about the time of the initial, main, and recovery phases, as well as the solar wind driver for each storm. Our process involved cross-referencing each storm from this list with the corresponding period in this list of sawtooth events from 1996-2007, (Cai & Clauer, 2009, 2013). If a storm in the first list involves a sawtooth event in the second list, we label the storm as a sawtooth storm; otherwise, it is labeled as a non-sawtooth storm.

Since simulations such as (Brambles et al., 2013) and (Varney et al., 2016), find that ionospheric O^+ outflow is only needed during storms with steady solar wind conditions to drive the sawtooth mode, this study is limited to the geomagnetic storms which are driven by CMEs. Also, to reduce the effect of the storm's intensity on this sawtooth/non-sawtooth comparison, this statistical analysis only examines moderate storms with $-150nT \leq Dst_{minimum} \leq -50nT$. In Figure 1, the minimum Dst of all CME moderate storms used in this study are plotted. The red and blue circles represent the sawtooth and non-sawtooth storms, respectively. The orange line shows the smoothed daily average of F10.7, the solar radio flux at 10.7 cm as an indicator of solar activity, during solar cycle 23, which spans from 1996 to 2008. It is observed that sawtooth events during moderate CME storms are observed in all the solar cycle's phases, however they are more common in the solar cycle's maximum phase with $180 s.f.u. < F10.7$ (or less common during the minimum phase with $F10.7 < 180 s.f.u.$). In Figure 1, the moderate CME storms include 158 sawtooth injections. In total, there are identified 4 teeth during the initial phase, 88 teeth during the storm main phase, 52 teeth during the early recovery phase, and 14 teeth during the long recovery phase.

The Fast Auroral Snapshot Explorer(FAST) spacecraft was launched in August 1996 to advance the study of auroral acceleration physics and magnetosphere-ionosphere coupling. FAST was placed into an elliptical polar orbit characterized by a period of 133 minutes, an inclination angle of 83°, a perigee altitude of approximately 350 km, and an apogee altitude of roughly 4175 km (Carlson et al., 1998). On the FAST spacecraft, the
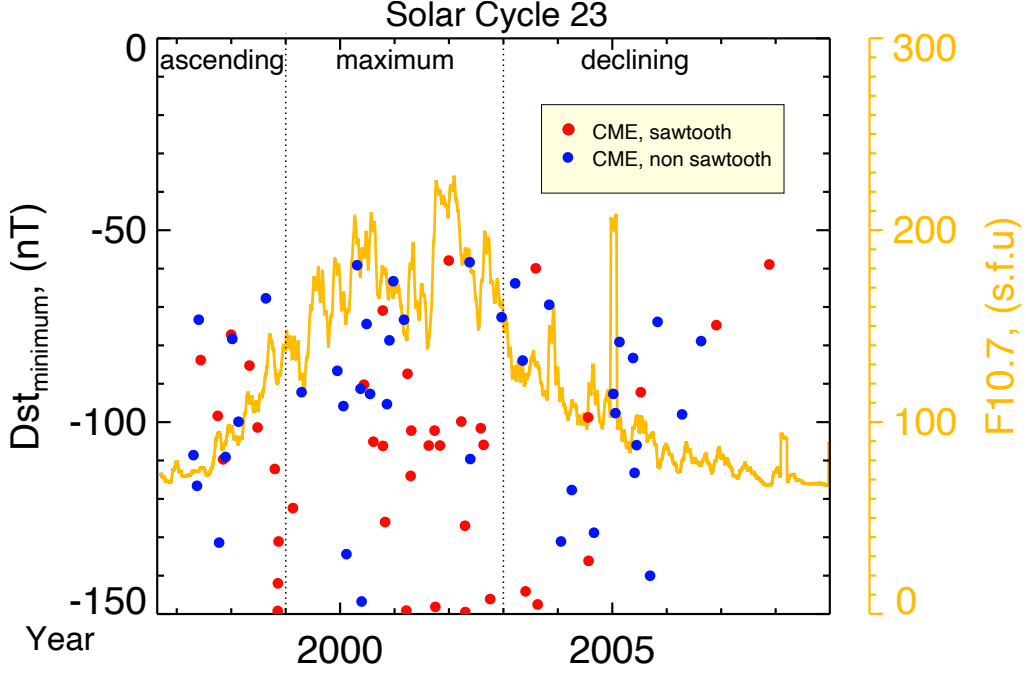
Figure 1. The scatter plot of the minimum Dst for CME sawtooth storms (red) and CME non-sawtooth storms(blue). The orange line shows the F10.7 indices for the 23rd solar cycle.

TEAMS instrument measured the 3-D distribution functions of particle species H^+, O^+, He^+ and He^{++}, (Klumpar et al., 2001). This study employs the recently recalibrated TEAMS L2 data [1] to calculate the ionospheric outflow flux of O^+ and H^+ ions with the following equation.

$$\Phi(m) = 2\pi \int_{E=10eV}^{E_{cutoff}} dE \int j(m, E, \alpha) |\sin(\alpha)\sin(\Delta\alpha)cos(\alpha)cos(\Delta\alpha)| d\alpha \qquad (1)$$

In equation 1, the variables α, $\Delta\alpha$, E, and $j(m, E, \alpha)$ represent the pitch angle in the center of the bin, half-width of the pitch angle bin which is $11.25°$, energy, and energy flux in the center of the bin for the species m, respectively. To exclude contributions from the magnetosphere and ram plasma within ionospheric outflow measurements, the energy flux is integrated over the energy range from $10eV$ to the dynamic cutoff energy, as described in detail by Hatch et al. (2020); Zhao et al. (2020); and Nowrouzi et al. (2023). This study utilizes data collected between 1500 km and 4200 km altitude of the northern and southern hemispheres. The net flux is normalized by mapping it to 300 km by using the IGRF model. Using the described methodology, the O^+ and H^+ outflow fluxes acquired from the northern and southern hemispheres are combined and calculated for the list's pre-storm and storm phase intervals.

Subsequently, the outflow rate (fluence) of O^+ and H^+ are quantified. The ion species fluence is determined by multiplying the averaged outflow flux and the surface area:

---

[1] most of the recalibrations were detailed in the Appendix section of Nowrouzi (2022)

$$fluence_{jk} = (\frac{\Sigma_{i=0}^{n_{jk}-1} flux_i}{n_{jk}}) \times A_{jk} \qquad (2)$$

Where A_{jk} is the area covered by bin jk at a mapped altitude of 300 km and n_{jk} is the number of samples in that bin. Outflow fluxes are grouped into storm phases for both sawtooth and non-sawtooth storms

Figures2 and 3 display the mapped net outflow fluxes of O^+ and H^+ in the polar region, respectively. The data in Figure 2 are divided into the three storm phases (initial, main, and recovery) in the three columns. The top panel illustrates the outflow flux along the spacecraft trajectory for Invariant Latitude (ILAT) values greater than $50°$ from all CME-driven storms during each storm phase. The black circles in these figures are spaced in $10°$ ILAT increments from all CME-driven storms during each storm phase. In the next panels, the data space is binned within the range of $50° < ILAT < 90°$ and $0 < MLT < 24$ into $40°$ ILAT bins, each with a width of $1°$ and 24 Magnetic Local Time (MLT) bins, each with a time width of 1 hour. Subsequently, the average ion outflow flux within each MLT-ILAT bin is calculated and assigned to that bin in the large dials. The number of measurements in each MLT-ILAT bin is presented in the smaller dials, plotted on the top of each big dial. The second panel illustrates the average outflow flux for all CME storms, which is shown in the trajectory panel. Then, the data plotted in the trajectory panel were divided into two groups, the sawtooth and non-sawtooth storms, and the averaged outflow flux of each group is plotted in the third and fourth panels.

3 Data Analysis and Discussion

In Figures 2 and 3, the lack of data samples in a few MLT-ILAT bins with lower latitudes (indicated in gray) limits the analysis of outflow fluxes to $60° < ILAT < 90°$. A visual comparison of the third and fourth panels shows that during the initial phase(left column), the O^+ and H^+ outflow fluxes in $70° < ILAT < 80°$ are stronger during non-sawtooth storms than during sawtooth storms. In the main phase, the different locations of the dominant outflow between sawtooth and non-sawtooth storms are considerable. During sawtooth storms, the peak outflow is observed in the dawn region, between 3 MLT and 8 MLT, mostly between $70°$ and $60°$ ILAT, while for non-sawtooth storms, the peak is closer to noon, spanning from 7 MLT to 13 MLT and between $80°$ and $65°$ ILAT. During the recovery phase, both sawtooth and non-sawtooth storms display the dayside cusp outflow from 7 MLT to 14 MLT, while the sawtooth storms show an additional large O^+ outflow on the dawnside from 2 MLT to 6 MLT, not observed in non-sawtooth storms. On the nightside, the high O^+ outflow in non-sawtooth storms shows a $\sim 5°$ equatorward shift of latitudinal location in sawtooth storms.

To quantitatively compare the outflow fluxes between sawtooth and non-sawtooth CME storms, the fluence of averaged outflow fluxes in each MLT-ILAT bin is calculated from equation 2, summed into three-hour MLT bins over the ILAT range from $60° < ILAT < 90°$ and displayed in Figure 4. From left to right: the O^+ fluence, the H^+ fluence, and the ratio fluences of O^+/H^+ are plotted as a function of MLT for the initial phase at the top, the main phase in the middle and the recovery phase at the bottom. The red and blue lines indicate outflow fluences during sawtooth and non-sawtooth storms, respectively. The error bars denote the standard deviation (SD).

In the initial phase, non-sawtooth storms show higher O^+ and H^+ outflow fluences than sawtooth storms in all MLT sectors, except before midnight, where sawtooth and non-sawtooth fluences are comparable in both O^+ and H^+ plots. The O^+ outflow fluence is up to 10 times larger in non-sawtooth storms than in sawtooth storms in some MLT sectors. This observation aligns with previous observational studies indicating a correlation between sawtooth events and solar wind, for instance, a study suggesting that
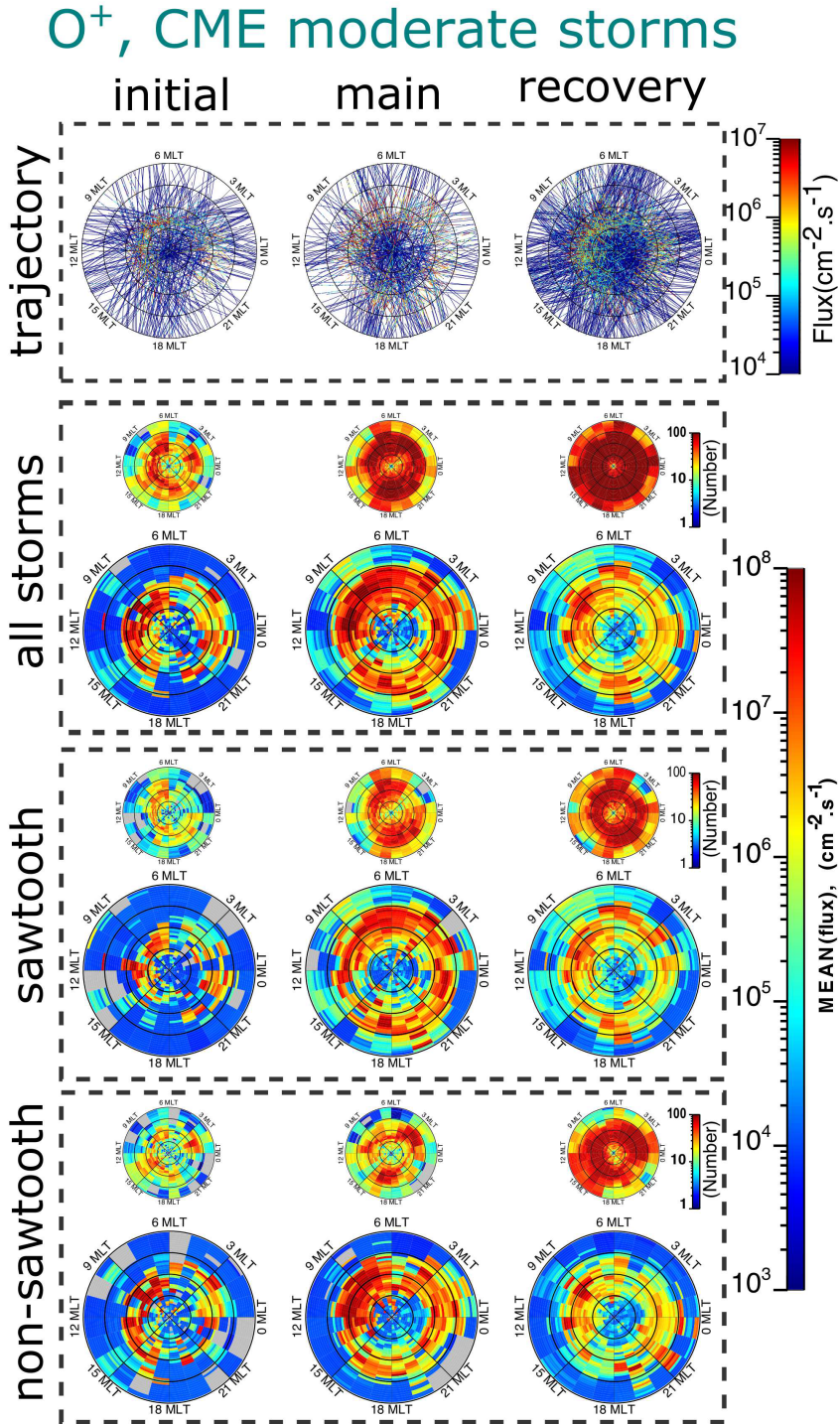
Figure 2. The top panel shows mapped O$^+$ outflow flux along the FAST trajectories for all moderate CME storms. Horizontally, columns display data during the initial, main, and recovery phases. The average of the first panel data is illustrated in the second panel. The third and fourth panels represent the averaged O$^+$ outflow flux from sawtooth storms and non-sawtooth storms, respectively. The big dials indicate the averaged outflow and the small dials show the number of data points in each bin.

H⁺, CME moderate storms
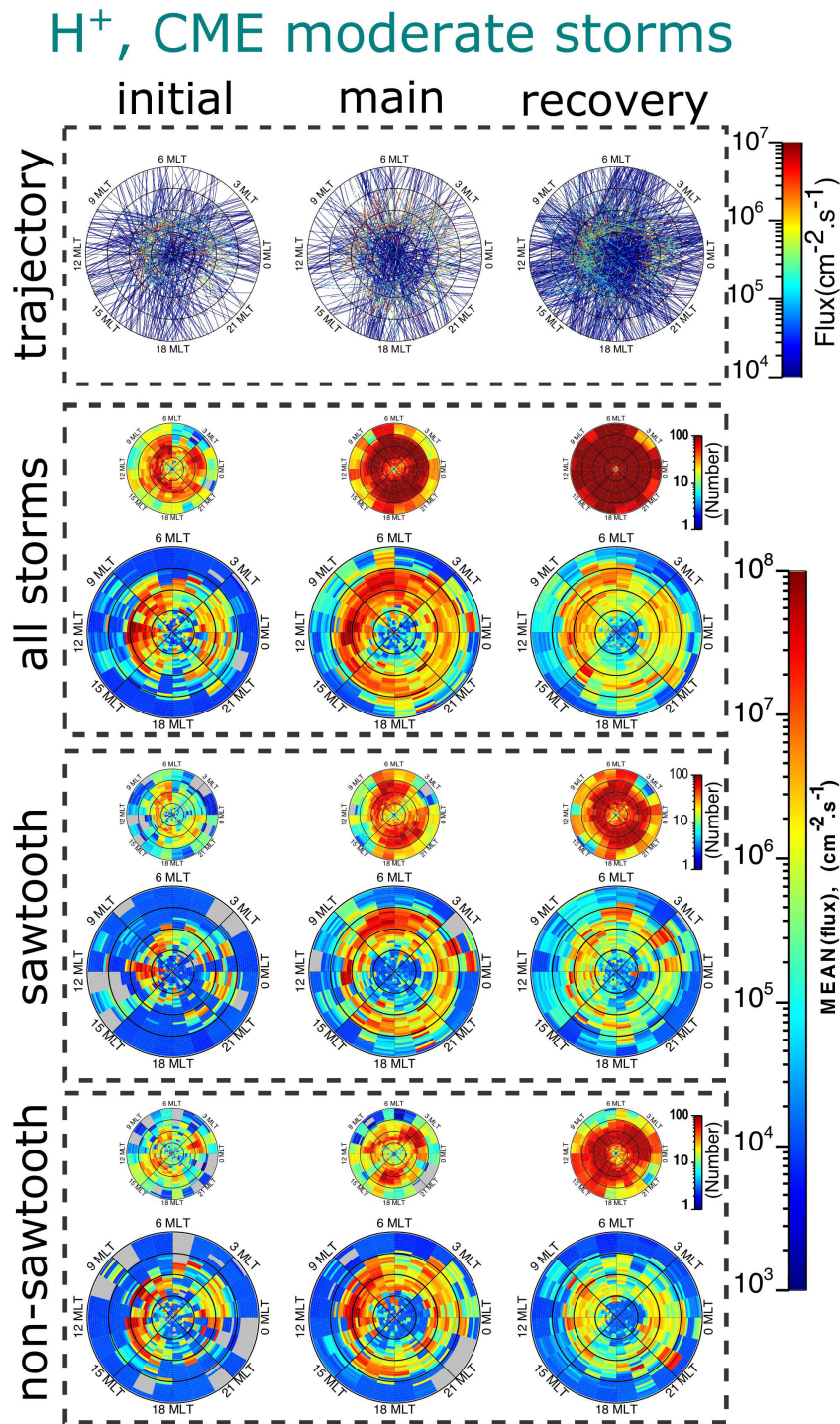
Figure 3. The mapped H⁺ outflow flux in the polar region. The format is the same as in Figure 2.
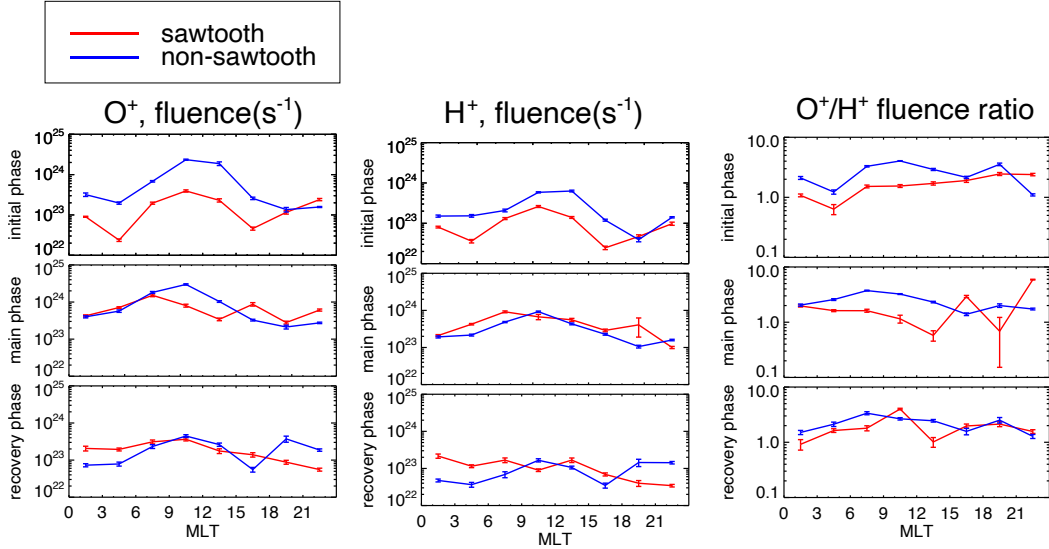
Figure 4. From left to right, the panels illustrate the O^+ and H^+ fluences and their ratio. Top to bottom, the panels display the mapped outflow flux fluences during the initial, main, and recovery phases as a function of MLT for sawtooth storms in red and non-sawtooth storms in blue.

sawtooth events do not occur when solar wind magnetic flux is higher than a threshold (Cai & Clauer, 2013).

During the main phase, the O^+ outflow fluence at noon is higher in non-sawtooth storms than in sawtooth storms, but, as noted above, the peak O^+ outflow is shifted toward dawn in sawtooth storms. During the recovery phase, the outflow on the dayside is comparable. This suggests that it is not significantly higher dayside O^+ outflow that is driving sawtooth events. However, it is possible that the enhanced dawnside outflow can populate the plasma sheet better than the outflow closer to noon, and so it has a greater effect.

Although during the main phase, sawtooth events display larger O^+ outflow before midnight than non-sawtooth events, during the recovery phase, this pattern is observed in the after-midnight MLT sectors. Before midnight, non-sawtooth storms show about 5 times higher O^+ outflow fluence than sawtooth storms. While enhanced nightside outflow could help to drive sawtooth events during the main phase, this observation argues against it being a cause during the recovery phase.

The observations for H^+ outflow fluence during storm phases are similar to the O^+ outflow fluence; however, the difference between sawtooth and non-sawtooth is weaker in the outflow fluence of H^+ than in the outflow fluence of O^+. In the ratio plot on the right, a higher O^+/H^+ is observed mainly during non-sawtooth storms than during sawtooth storms. However, the notable exceptions in the pre-midnight MLT sectors are considerable.

4 Summary and Conclusions

This paper performed a statistical analysis on 11 years of FAST/TEAMS charged particle data from 1996 through 2007, focusing on CME-driven moderate storms. The

objective of the study was to explore any observational evidence showing differences in ionospheric outflow between sawtooth and non-sawtooth storms that support the role of O^+ outflow in driving sawtooth oscillations. The observations indicate that the location of high ionospheric outflow differs between sawtooth and non-sawtooth events. This study reveals that:

1- In the initial phase, the non-sawtooth storms generate larger O^+ outflow than sawtooth storms in most MLT sectors. Since the initial phase outflow would be the first to reach the plasma sheet during a storm, this suggests that, at least in the early phase of a storm, the cusp outflow is not important in triggering the sawtooth oscillations or may even suggest that the initial phase outflow from the cusp, if anything, suppresses sawtooth oscillations.

2- During the main and recovery phase, the O^+ outflow fluence in the nightside region is higher in sawtooth storms than in non-sawtooth storms during the pre-midnight sector of the main phase and the post-midnight sector of the recovery phase and significantly lower during the post-midnight sector of the recovery phase.

3- During the main and recovery phases, while the outflow at noon is lower during sawtooth storms, the peak of the O^+ outflow is shifted toward the dawn sector in sawtooth storms. This suggests that while the levels of peak O^+ outflow are comparable between sawtooth and non-sawtooth storms, their spatial distribution differs. Consequently, this difference in location may help with access to the plasma sheet.

In summary, there are significant differences in the outflow patterns between storms with sawtooth oscillations and storms without. However, the observations do not unambiguously support one model over another, with differences observed both on the dayside and the nightside. The most compelling difference is that the location of the peak dayside outflow is shifted significantly towards dawn in the sawtooth storms, and we suggest exploring the impacts of this difference in future simulations.

5 Acknowledgments

6 Open Research

All the data used in creating this manuscript is publicly available. The OMNI data can be accessed at `https://spdf.gsfc.nasa.gov/pub/data/omni/low_res_omni`. The recalibrated FAST(TEAMS) can be found at `https://spdf.gsfc.nasa.gov/pub/data/fast/teams/l2/pa/`. All figures were generated using IDL version $8.9.0 (Linux.x86_64m64)$ copyright 2023, and the software is available under the license of L3 Harris Geospatial Solutions at `https://www.nv5geospatialsoftware.com/Products/IDL`.

References

Belian, R. D., & Cayton, T. E. (1989, January). The effects of the major solar storm of February 1986 as seen by energetic particle detector on three nearly equidistant geosynchronous satellites. *Nagoya University Research Institute of Atmospherics Proceedings*, *36*(2), 127-136.

Belian, R. D., Cayton, T. E., & Reeves, G. D. (1995). Quasi-Periodic Global Substorm Generated Flux Variations Observed at Geosynchronous Orbit. In *Space plasmas: Coupling between small and medium scale processes* (p. 143-148). American Geophysical Union (AGU). Retrieved from

https://agupubs.onlinelibrary.wiley.com/doi/abs/10.1029/GM086p0143
doi: https://doi.org/10.1029/GM086p0143

Borovsky, J. E. (2004). Global sawtooth oscillations of the magnetosphere. *Eos, Transactions American Geophysical Union*, *85*(49), 525-525. Retrieved from https://agupubs.onlinelibrary.wiley.com/doi/abs/10.1029/2004EO490009 doi: https://doi.org/10.1029/2004EO490009

Borovsky, J. E., Nemzek, R. J., & Belian, R. D. (1993). The occurrence rate of magnetospheric-substorm onsets: Random and periodic substorms. *Journal of Geophysical Research: Space Physics*, *98*(A3), 3807-3813. Retrieved from https://agupubs.onlinelibrary.wiley.com/doi/abs/10.1029/92JA02556 doi: https://doi.org/10.1029/92JA02556

Brambles, O. J., Lotko, W., Zhang, B., Ouellette, J., Lyon, J., & Wiltberger, M. (2013). The effects of ionospheric outflow on ICME and SIR driven sawtooth events. *Journal of Geophysical Research: Space Physics*, *118*(10), 6026-6041. Retrieved from https://agupubs.onlinelibrary.wiley.com/doi/abs/10.1002/jgra.50522 doi: https://doi.org/10.1002/jgra.50522

Brambles, O. J., Lotko, W., Zhang, B., Wiltberger, M., Lyon, J., & Strangeway, R. J. (2011). Magnetosphere Sawtooth Oscillations Induced by Ionospheric Outflow. *Science*, *332*(6034), 1183-1186. Retrieved from https://www.science.org/doi/abs/10.1126/science.1202869 doi: 10.1126/science.1202869

Cai, X., & Clauer, C. R. (2009). Investigation of the period of sawtooth events. *Journal of Geophysical Research: Space Physics*, *114*(A6). Retrieved from https://agupubs.onlinelibrary.wiley.com/doi/abs/10.1029/2008JA013764 doi: https://doi.org/10.1029/2008JA013764

Cai, X., & Clauer, C. R. (2013). Magnetospheric sawtooth events during the solar cycle 23. *Journal of Geophysical Research: Space Physics*, *118*(10), 6378-6388. Retrieved from https://agupubs.onlinelibrary.wiley.com/doi/abs/10.1002/2013JA018819 doi: https://doi.org/10.1002/2013JA018819

Cai, X., Henderson, M. G., & Clauer, C. R. (2006). A statistical study of magnetic dipolarization for sawtooth events and isolated substorms at geosynchronous orbit with GOES data. *Annales Geophysicae*, *24*(12), 3481–3490. Retrieved from https://angeo.copernicus.org/articles/24/3481/2006/ doi: 10.5194/angeo-24-3481-2006

Cai, X., Zhang, J.-C., Clauer, C. R., & Liemohn, M. W. (2011). Relationship between sawtooth events and magnetic storms. *Journal of Geophysical Research: Space Physics*, *116*(A7). Retrieved from https://agupubs.onlinelibrary.wiley.com/doi/abs/10.1029/2010JA016310 doi: https://doi.org/10.1029/2010JA016310

Carlson, C. W., Pfaff, R. F., & Watzin, J. G. (1998). The Fast Auroral SnapshoT (FAST) Mission. *Geophysical Research Letters*, *25*(12), 2013-2016. Retrieved from https://agupubs.onlinelibrary.wiley.com/doi/abs/10.1029/98GL01592 doi: https://doi.org/10.1029/98GL01592

Cully, C. M., Donovan, E. F., Yau, A. W., & Arkos, G. G. (2003). Akebono/Suprathermal Mass Spectrometer observations of low-energy ion outflow: Dependence on magnetic activity and solar wind conditions. *Journal of Geophysical Research: Space Physics*, *108*(A2). Retrieved from https://agupubs.onlinelibrary.wiley.com/doi/abs/10.1029/2001JA009200 doi: https://doi.org/10.1029/2001JA009200

DeJong, A. D., Ridley, A. J., & Clauer, C. R. (2008). Balanced reconnection intervals: four case studies. *Annales Geophysicae*, *26*(12), 3897–3912. Retrieved from https://angeo.copernicus.org/articles/26/3897/2008/ doi: 10.5194/angeo-26-3897-2008

Hatch, S. M., Moretto, T., Lynch, K. A., Laundal, K. M., Gjerloev, J. W., & Lund, E. J. (2020). The Relationship Between Cusp Region Ion Out-

flows and East-West Magnetic Field Fluctuations at 4,000-km Altitude. *Journal of Geophysical Research: Space Physics*, *125*(3), e2019JA027454. Retrieved from `https://agupubs.onlinelibrary.wiley.com/doi/abs/10.1029/2019JA027454` (e2019JA027454 10.1029/2019JA027454) doi: https://doi.org/10.1029/2019JA027454

Henderson, M. G. (2004). The May 2–3, 1986 CDAW-9C interval: A sawtooth event. *Geophysical Research Letters*, *31*(11). Retrieved from `https://agupubs.onlinelibrary.wiley.com/doi/abs/10.1029/2004GL019941` doi: https://doi.org/10.1029/2004GL019941

Henderson, M. G., Reeves, G. D., Skoug, R., Thomsen, M. F., Denton, M. H., Mende, S. B., . . . Singer, H. J. (2006). Magnetospheric and auroral activity during the 18 April 2002 sawtooth event. *Journal of Geophysical Research: Space Physics*, *111*(A1). Retrieved from `https://agupubs.onlinelibrary.wiley.com/doi/abs/10.1029/2005JA011111` doi: https://doi.org/10.1029/2005JA011111

Hones Jr., E. W., Pytte, T., & West Jr., H. I. (1984). Associations of geomagnetic activity with plasma sheet thinning and expansion: A statistical study. *Journal of Geophysical Research: Space Physics*, *89*(A7), 5471-5478. Retrieved from `https://agupubs.onlinelibrary.wiley.com/doi/abs/10.1029/JA089iA07p05471` doi: https://doi.org/10.1029/JA089iA07p05471

Huang, C.-S. (2011). Relation between magnetotail magnetic flux and changes in the solar wind during sawtooth events: Toward resolving the controversy of whether all substorm onsets are externally triggered. *Journal of Geophysical Research: Space Physics*, *116*(A4). Retrieved from `https://agupubs.onlinelibrary.wiley.com/doi/abs/10.1029/2010JA016371` doi: https://doi.org/10.1029/2010JA016371

Huang, C.-S., & Cai, X. (2009). Magnetotail total pressure and lobe magnetic field at onsets of sawtooth events and their relation to the solar wind. *Journal of Geophysical Research: Space Physics*, *114*(A4). Retrieved from `https://agupubs.onlinelibrary.wiley.com/doi/abs/10.1029/2008JA013807` doi: https://doi.org/10.1029/2008JA013807

Huang, C.-S., Foster, J. C., Reeves, G. D., Le, G., Frey, H. U., Pollock, C. J., & Jahn, J.-M. (2003). Periodic magnetospheric substorms: Multiple space-based and ground-based instrumental observations. *Journal of Geophysical Research: Space Physics*, *108*(A11). Retrieved from `https://agupubs.onlinelibrary.wiley.com/doi/abs/10.1029/2003JA009992` doi: https://doi.org/10.1029/2003JA009992

Kistler, L. M., Mouikis, C. G., Cao, X., Frey, H., Klecker, B., Dandouras, I., . . . Lucek, E. (2006). Ion composition and pressure changes in storm time and nonstorm substorms in the vicinity of the near-Earth neutral line. *Journal of Geophysical Research: Space Physics*, *111*(A11). Retrieved from `https://agupubs.onlinelibrary.wiley.com/doi/abs/10.1029/2006JA011939` doi: https://doi.org/10.1029/2006JA011939

Kistler, L. M., Mouikis, C. G., Klecker, B., & Dandouras, I. (2010). Cusp as a source for oxygen in the plasma sheet during geomagnetic storms. *Journal of Geophysical Research: Space Physics*, *115*(A3). Retrieved from `https://agupubs.onlinelibrary.wiley.com/doi/abs/10.1029/2009JA014838` doi: https://doi.org/10.1029/2009JA014838

Kitamura, K., Kawano, H., Ohtani, S.-i., Yoshikawa, A., & Yumoto, K. (2005). Local time distribution of low and middle latitude ground magnetic disturbances at sawtooth injections of 18–19 April 2002. *Journal of Geophysical Research: Space Physics*, *110*(A7). Retrieved from `https://agupubs.onlinelibrary.wiley.com/doi/abs/10.1029/2004JA010734` doi: https://doi.org/10.1029/2004JA010734

Klumpar, D., Möbius, E., Kistler, L., Popecki, M., Hertzberg, E., Crocker, K., . . .

Hovestadt, D. (2001). The Time-of-Flight Energy, Angle, Mass Spectrograph (Teams) Experiment for Fast. *Space science reviews*, *98*(1-2), 197–219.

Lee, D.-Y., Lyons, L. R., Kim, K. C., Baek, J.-H., Kim, K.-H., Kim, H.-J., ... Han, W. (2006). Repetitive substorms caused by Alfvénic waves of the interplanetary magnetic field during high-speed solar wind streams. *Journal of Geophysical Research: Space Physics*, *111*(A12). Retrieved from `https://agupubs.onlinelibrary.wiley.com/doi/abs/10.1029/2006JA011685` doi: https://doi.org/10.1029/2006JA011685

Lee, D.-Y., Lyons, L. R., & Yumoto, K. (2004). Sawtooth oscillations directly driven by solar wind dynamic pressure enhancements. *Journal of Geophysical Research: Space Physics*, *109*(A4). Retrieved from `https://agupubs.onlinelibrary.wiley.com/doi/abs/10.1029/2003JA010246` doi: https://doi.org/10.1029/2003JA010246

Liao, J., Cai, X., Kistler, L. M., Clauer, C. R., Mouikis, C. G., Klecker, B., & Dandouras, I. (2014). The relationship between sawtooth events and O+ in the plasma sheet. *Journal of Geophysical Research: Space Physics*, *119*(3), 1572-1586. Retrieved from `https://agupubs.onlinelibrary.wiley.com/doi/abs/10.1002/2013JA019084` doi: https://doi.org/10.1002/2013JA019084

Liao, J., Kistler, L. M., Mouikis, C. G., Klecker, B., Dandouras, I., & Zhang, J.-C. (2010). Statistical study of O+ transport from the cusp to the lobes with Cluster CODIF data. *Journal of Geophysical Research: Space Physics*, *115*(A12). Retrieved from `https://agupubs.onlinelibrary.wiley.com/doi/abs/10.1029/2010JA015613` doi: https://doi.org/10.1029/2010JA015613

Lund, E. J., Nowrouzi, N., Kistler, L. M., Cai, X., & Frey, H. U. (2018). On the Role of Ionospheric Ions in Sawtooth Events. *Journal of Geophysical Research: Space Physics*, *123*(1), 665-684. Retrieved from `https://agupubs.onlinelibrary.wiley.com/doi/abs/10.1002/2017JA024378` doi: https://doi.org/10.1002/2017JA024378

Lyon, J., Fedder, J., & Mobarry, C. (2004). The Lyon–Fedder–Mobarry (LFM) global MHD magnetospheric simulation code. *Journal of Atmospheric and Solar-Terrestrial Physics*, *66*(15), 1333-1350. Retrieved from `https://www.sciencedirect.com/science/article/pii/S1364682604001439` (Towards an Integrated Model of the Space Weather System) doi: https://doi.org/10.1016/j.jastp.2004.03.020

Nowrouzi, N. (2022). *Ionospheric O+ and H+ Outflow During Geomagnetic Storms* (Doctoral dissertation, University of New Hampshire). Retrieved from `https://scholars.unh.edu/dissertation/2722`

Nowrouzi, N., Kistler, L. M., Zhao, K., Lund, E. J., Mouikis, C., Payne, G., & Klecker, B. (2023). The Variation of Ionospheric O+ and H+ Outflow on Storm Timescales. *Journal of Geophysical Research: Space Physics*, *128*. Retrieved from `https://agupubs.onlinelibrary.wiley.com/doi/10.1029/2023JA031786` doi: https://doi.org/10.1029/2023JA031786

Ouellette, J. E., Brambles, O. J., Lyon, J. G., Lotko, W., & Rogers, B. N. (2013). Properties of outflow-driven sawtooth substorms. *Journal of Geophysical Research: Space Physics*, *118*(6), 3223-3232. Retrieved from `https://agupubs.onlinelibrary.wiley.com/doi/abs/10.1002/jgra.50309` doi: https://doi.org/10.1002/jgra.50309

Reeves, G., Thomsen, M., Henderson, M., Skoug, R., Borovsky, J., Jahn, J., ... others (2002). Global Sawtooth Activity in the April 2002 Geomagnetic Storm. In *Agu fall meeting abstracts* (Vol. 2002, pp. SA12A–05).

Russell, C. T., & McPherron, R. L. (1973, Nov 01). The magnetotail and substorms. *Space Science Reviews*, *15*(2), 205-266. Retrieved from `https://doi.org/10.1007/BF00169321` doi: 10.1007/BF00169321

Sergeev, V. A., Pellinen, R. J., & Pulkkinen, T. I. (1996, Feb 01). Steady magnetospheric convection: A review of recent results. *Space Science Reviews*, *75*(3),

551-604. Retrieved from https://doi.org/10.1007/BF00833344 doi: 10 .1007/BF00833344

Sharp, R. D., Johnson, R. G., Shelley, E. G., & Harris, K. K. (1974, January). Energetic O$^+$ ions in the magnetosphere. *Journal of Geophysical Research: Space Physics*, *79*(13), 1844. doi: 10.1029/JA079i013p01844

Shelley, E. G., Johnson, R. G., & Sharp, R. D. (1972). Satellite observations of energetic heavy ions during a geomagnetic storm. *Journal of Geophysical Research (1896-1977)*, *77*(31), 6104-6110. Retrieved from https:// agupubs.onlinelibrary.wiley.com/doi/abs/10.1029/JA077i031p06104 doi: https://doi.org/10.1029/JA077i031p06104

Troshichev, O., & Janzhura, A. (2009). Relationship between the PC and AL indices during repetitive bay-like magnetic disturbances in the auroral zone. *Journal of atmospheric and solar-terrestrial physics*, *71*(12), 1340-1352.

Varney, R. H., Wiltberger, M., Zhang, B., Lotko, W., & Lyon, J. (2016). Influence of ion outflow in coupled geospace simulations: 2. Sawtooth oscillations driven by physics-based ion outflow. *Journal of Geophysical Research: Space Physics*, *121*(10), 9688-9700. Retrieved from https:// agupubs.onlinelibrary.wiley.com/doi/abs/10.1002/2016JA022778 doi: https://doi.org/10.1002/2016JA022778

Wang, X., Chen, Y., & Tóth, G. (2022). Simulation of Magnetospheric Sawtooth Oscillations: The Role of Kinetic Reconnection in the Magnetotail. *Geophysical Research Letters*, *49*(15), e2022GL099638. Retrieved from https:// agupubs.onlinelibrary.wiley.com/doi/abs/10.1029/2022GL099638 (e2022GL099638 2022GL099638) doi: https://doi.org/10.1029/2022GL099638

Yau, A. W., & André, M. (1997, Apr 01). Sources of Ion Outflow in the High Latitude Ionosphere. *Space Science Reviews*, *80*(1), 1-25. Retrieved from https:// doi.org/10.1023/A:1004947203046 doi: 10.1023/A:1004947203046

Yau, A. W., Peterson, W. K., & Shelley, E. G. (1988, jan). Quantitative parametrization of energetic ionospheric ion outflow. *Geophysical Monograph Series*, *44*, 211-217. doi: 10.1029/GM044p0211

Zhang, B., Brambles, O. J., Lotko, W., & Lyon, J. G. (2020). Is Nightside Outflow Required to Induce Magnetospheric Sawtooth Oscillations. *Geophysical Research Letters*, *47*(6), e2019GL086419. Retrieved from https:// agupubs.onlinelibrary.wiley.com/doi/abs/10.1029/2019GL086419 (e2019GL086419 10.1029/2019GL086419) doi: https://doi.org/10.1029/ 2019GL086419

Zhao, K., Kistler, L. M., Lund, E. J., Nowrouzi, N., Kitamura, N., & Strangeway, R. J. (2020). Factors Controlling O+ and H+ Outflow in the Cusp During a Geomagnetic Storm: FAST/TEAMS Observations. *Geophysical Research Letters*, *47*(11), e2020GL086975. Retrieved from https:// agupubs.onlinelibrary.wiley.com/doi/abs/10.1029/2020GL086975 (e2020GL086975 2020GL086975) doi: https://doi.org/10.1029/2020GL086975